refinement or a direct-methods procedure independent of the satellite reflections. This, at first sight surprising, result can be understood from the special nature of intergrowth compounds. The two subsystems coexist in a single thermodynamic phase and part of the satellite intensity due to the modulation is already contained in the main reflections. This information allowed the refinement of modulation parameters on main reflections only (Kato, 1990), but it is insufficient to reveal the modulation amplitudes in a Fourier synthesis (Fig. 1). The method proposed here allows one to calculate the satellite structure factors from the main reflections with sufficient accuracy to determine the modulation from a Fourier map (Fig. 2).

Phases of the satellite reflections can be obtained as described earlier (Fan, van Smaalen, Lam & Beurskens, 1993). For their magnitudes to be determined, a crucial step is that the functions $\theta_{sat}(\mathbf{H}_s)$ and $\theta_{main}(\mathbf{H}_s)$ can both be determined from the main reflections alone [(15), (16) and (19)]. Applications are given to the inorganic misfit layer compounds $(LaS)_{1.14}NbS_2$ and $(PbS)_{1.18}TiS_2$. The Fourier map calculated with the main reflections and the satellite reflections generated in the direct-methods procedure is found to be indistinguishable from the Fourier synthesis using experimental amplitudes for all reflections combined with phases from the refinement (Figs. 2 and 3). This shows the structure factors of the satellite reflections calculated with (15) to be sufficiently accurate to determine the modulations in these composite crystals.

References

FAN, H. F., VAN SMAALEN, S., LAM, E. J. W. & BEURSKENS, P. T. (1993). *Acta Cryst.* A**49**, 704–708.

HAO, Q., LIU, Y. W. & FAN, H. F. (1987). *Acta Cryst.* A**43**, 820–824.

JANNER, A. & JANSSEN, T. (1980). *Acta Cryst.* A**36**, 408–415.

KATO, K. (1990). *Acta Cryst.* B**46**, 39–44.

PETRICEK, V., MALY, K., COPPENS, P., BU, X., CISAROVA, I. & FROST-JENSEN, A. (1991). *Acta Cryst.* A**47**, 210–216.

SMAALEN, S. VAN (1991). *J. Phys. Condens. Matter*, **3**, 1247–1263.

SMAALEN, S. VAN (1992). *Mater. Sci. Forum*, **100&101**, 173–222.

SMAALEN, S. VAN, MEETSMA, A., WIEGERS, G. A. & DE BOER, J. L. (1991). *Acta Cryst.* B**47**, 314–325.

WIEGERS, G. A. & MEERSCHAUT, A. (1992). *Mater. Sci. Forum*, **100&101**, 101–172.

YAMAMOTO, A. (1982). *Acta Cryst.* A**38**, 87–92.

YAMAMOTO, A. (1992). *Acta Cryst.* A**48**, 476–483.

Acta Cryst. (1994). A**50**, 515–526

Quasicrystals and their Approximants: Dodecahedral Local Ordering *Versus* Canonical-Cell Description

BY V. E. DMITRIENKO

A. V. Shubnikov Institute of Crystallography, 117333 Moscow, Russia

(*Received* 7 *June* 1993; *accepted* 14 *December* 1993)

Abstract

Two models of icosahedral quasicrystals are compared and connected. These are canonical-cell ordering (CCO) over medium-length scales (about 10 Å and more) and dodecahedral local ordering (DLO), which describes interatomic arrangements. In the DLO model, each atom is surrounded by closest neighbours positioned at several vertices of a regular pentagon-dodecahedron; of the 20 vertices of any dodecahedron, only a few can be occupied simultaneously without conflict (eight at most). Some icosahedral quasicrystals and their crystalline approximants exhibit DLO as the main structure motif at atomic scales. DLO networks are formally described using an unconventional projection of a six-dimensional lattice. It is shown that most DLO configurations (but not all of them!) can be constructed from small atomic size canonical cells that are a factor of τ^3 smaller than the original ones. Two of the small canonical cells have the forms of distorted tetrahedra. It is also shown that DLO produces naturally the two most popular decorations of the Ammann rhombohedra: the edge decoration and the vertex-face decoration. Moreover, both decorations can be identified inside the same approximant. For medium-range distances, DLO leads to CCO with special decorations of the canonical cells. Therefore, the ordering in quasicrystals and in their approximants can be constructed as a hierarchy of dodecahedral ordering (or a hierarchy of canonical cells). It is shown that within the DLO model there may be an additional ordering of closest neighbours that leads to the transition between quasicrystals with primitive and face-centred lattices. The DLO-based duality between α-AlMnSi and Al_5Li_3Cu approximants is demonstrated. Possible physi-

cal reasons for DLO are considered. Some intrinsic features and difficulties of the DLO and CCO models (frustrations, disorder *etc.*) are discussed.

1. Introduction

Since the discovery of quasicrystals, much effort has been expended in understanding their atomic ordering. Even before their discovery, it was recognized by Penrose (1979) and Mackay (1981) that the quasicrystalline ordering should be a hierarchy of similar units; that is, the ordering should reproduce itself at ever larger scales (*inflation*). For icosahedral quasicrystals, the inflation factor should be equal to τ or τ^3 [τ is the golden mean, $\tau = 1 + 5^{1/2}/2$]. This type of ordering is exemplified by Penrose tilings but the typical structural units of three-dimensional Penrose tilings (prolate and oblate Ammann rhombohedra) are too large to describe an interatomic ordering and their atomic decorations are not obvious. Earlier, it was widely believed that a hierarchy of icosahedral units could produce the quasicrystalline ordering; however, the analysis of known crystal approximants showed that only a minority of the atoms have icosahedrally arranged nearest neighbours. It seems that the general principles of quasicrystalline structures have been understood better than the reasons for their growth from real atoms (Guyot, Kramer & de Boissieu, 1991; Kléman, 1989; Steurer, 1990). But a more complete understanding is urgently needed because these reasons should be common to various systems (quasicrystals, metallic glasses, Frank–Kasper phases *etc.*).

In a recent fundamental paper (Henley, 1991), several canonical cells are used as structure units for icosahedral quasicrystals. Each cell can be constructed from the Ammann rhombohedra. Quasicrystals and their approximants can be produced using either deterministic or partly random *canonical-cell ordering* (CCO). The generic size of the cells (the length of their shortest edges) is more than 10 Å and the problem of the atomic decoration still remains open.

On the other hand, it is found (Dmitrienko, 1992, 1993) that most atoms in crystalline approximants (and perhaps in quasicrystals) have *dodecahedral* local arrangements, so that the closest neighbours are positioned at a few vertices of a small pentagon-dodecahedron. This model is based both on the structure of a very simple approximant (Dmitrienko, 1990) and on the local ordering, experimentally determined in AlMnSi quasicrystals by Janot, Dubois, Pannetier, de Boissieu & Fruchart (1988), in AlFeCu quasicrystals by Cornier-Quiquandon, Quivy, Lefebre, Elkaim, Heger, Katz & Gratias (1991) and in AlPdMn quasicrystals by Boudard, de Boissieu, Janot, Heger, Beeli, Nissen, Vincent, Ibberson, Audier & Dubois (1992). It is shown below that, when continued on larger scales, such *dodecahedral local ordering* (DLO) produces the Ammann rhombohedra and large units with icosahedral symmetry. At the same time, DLO can produce *frustrated* positions; among these are positions with icosahedral local coordinations. Therefore, it is not surprising that those positions are rather minor and that in the real crystals they may be empty (as in Al_5Li_3Cu).

An aim of the present paper is to connect the dodecahedral local ordering and the canonical-cell ordering, but the global aim is to find a natural crystallographic background for rather baroque units of modern quasicrystallography. A short discussion of DLO in crystals and quasicrystals is given in §§ 2 and 3. The *dodecahedral* projection scheme (different from the conventional *icosahedral* one) is described in § 4. In § 5, it is shown that DLO can be constructed from small atomic size canonical cells. Then, in § 6, we obtain the decorated Ammann rhombohedra and the canonical cells as a natural result of the DLO. Such a relationship between DLO and CCO produces the τ^3 self-similarity of quasicrystalline ordering; perhaps the similarity of this type can be extended for ever larger scales *ad infinitum*. In § 7, an additional ordering of DLO networks is considered as a possible mechanism of the transition between *primitive* and *face-centred* quasicrystals. The discussion of different aspects of DLO in real structures can be found in §§ 8, 9 and 10. This paper is an introductory one and therefore some of the relevant problems are discussed very briefly: they will be considered in detail elsewhere.

2. Dodecahedral local ordering in simple structures

The question of the local arrangement of atoms in quasicrystals is one of the most important since the discovery of quasicrystals, but its complete solution is still absent. In our recent papers (Dmitrienko, 1992, 1993), DLO was suggested as the main structure motif in quasicrystals. In this and subsequent sections, we illustrate DLO using well known crystal structures and later, in §8, we discuss some physical reasons for such ordering.

In the beginning, we restrict ourself to the simplest cubic approximants of quasicrystals (see Figs. 1*a* and *b*) because from simple structures we can better understand the reasons for typical atomic arrangements. A cubic approximant will be labelled by two Fibonacci numbers $\langle F_{n+1}/F_n\rangle$ if in this crystal the strongest pseudo-fivefold reflections have the Miller indices $\{F_{n+1}, 0, F_n\}$ (Dmitrienko, 1990). Six reflections of this type can be used as the basis for other Bragg reflections. In our notation, the well known structures Al_5Li_3Cu and α-AlMnSi are $\langle 5/3\rangle$ approximants. The ratio of two lattice constants a_{n+1} and a_n of two succeeding approximants $\langle F_{n+2}/F_{n+1}\rangle$ and $\langle F_{n+1}/F_n\rangle$ is close to the golden mean τ [$\tau = (1 + 5^{1/2})/2 = 1.618034\ldots$]. Note that there is another labelling scheme (Elser & Henley, 1985) in which the α-AlMnSi crystal is labelled $\langle 1/1\rangle$ but

in this case we have an unnatural notation for smaller approximants.

It is well known that there is a relationship between orientations of the symmetry axes in icosahedral quasicrystals and their cubic approximants. If we inscribe a dodecahedron into a cube, eight of its threefold axes coincide with eight $\langle 111 \rangle$ cubic axes. The other twelve threefold axes are parallel to the $\langle 01\tau^2 \rangle$ directions; these directions are not symmetry axes of cubic crystals but the cubic approximants of quasicrystals have approximate threefold symmetry relative to these directions. Therefore, the $\langle 01\tau^2 \rangle$ directions are referred to as pseudo-threefold directions. In any cubic approximant, there are also six $\langle 001 \rangle$ twofold axes, twenty-four $\langle 1\tau\tau^2 \rangle$ pseudo-twofold axes and twelve $\langle 10\tau \rangle$ pseudo-fivefold axes.

One type of the $\langle 2/1 \rangle$ approximant (Dmitrienko, 1990) is exemplified by the FeSi structure (Fig. 1*a*). The space group of this structure is $P2_13$; its unit cell contains eight atoms in 4(*a*) positions (x,x,x) at the threefold axes: four *L* atoms and four *S* atoms. For the idealized structure of this approximant, the dimensionless coordinates of *L* and *S* atoms in the unit cell are

$$x_L = 1/(4\tau) \simeq 0.155; \quad x_S = 1 - x_L \simeq 0.845. \quad (1)$$

In such a structure, each *L* atom (large circles in Fig. 1*a*) is surrounded by seven *S* atoms (small circles in Fig. 1*a*) positioned at seven vertices of an ideal dodecahedron and *vice versa*. The dodecahedra have the same orientation; only one of them is shown for the atom in the upper-left corner of Fig. 1*a*.

In other words, all shortest *L*-*S* bonds are directed along either threefold $\langle 111 \rangle$ or pseudo-threefold $\langle 01\tau^2 \rangle$ directions. The second atomic shell contains six atoms of the same sort as the central one; the shortest *L*-*L* and *S*-*S* bonds are parallel to the pseudo-twofold $\langle 1\tau\tau^2 \rangle$ directions. The closest *L*-*S* distances are equal to c_{-3}, whereas the closest *L*-*L* (or *S*-*S*) distances are $2/3^{1/2}$ times longer (b_{-3}). The definitions of c_{-3} and b_{-3} are given at the beginning of §5. In the dimensionless coordinates, these two distances are equal to $3^{1/2}/(2\tau)$ and $1/\tau$, respectively. Thus, there is a compact cluster of seven *L* atoms and seven *S* atoms with threefold symmetry where the central atom is surrounded by 13 atoms. Two types of rhombohedron can be found in this structure: oblate [rhombohedral angle $\alpha_{ob} = \arccos(-1/3) \simeq 109° 28'$] and prolate [$\alpha_{pr} = \pi - \alpha_{ob} \simeq 70° 31'$). The faces of both rhombohedra are of the same form and they can match together; the unit cell may be divided into four prolate and four oblate rhombohedra (these rhombohedra should not be confused with the Ammann rhombohedra considered in § 6).

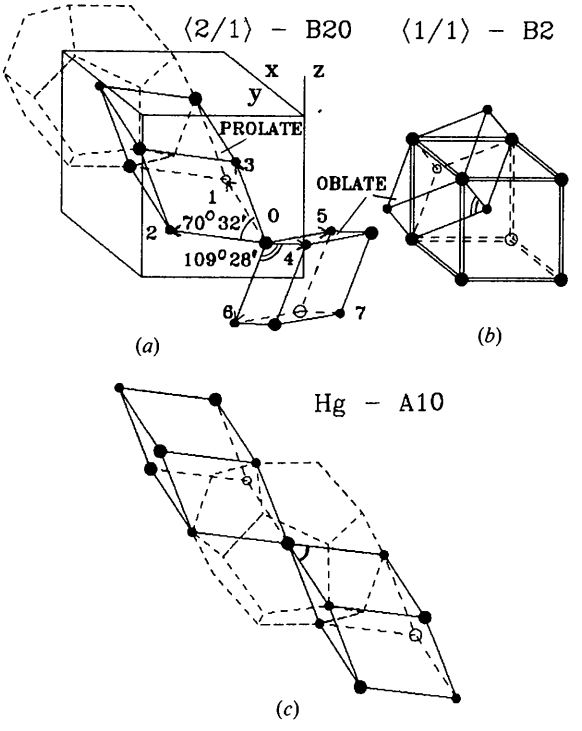

Fig. 1. Dodecahedral local ordering in crystals. (*a*) The $\langle 2/1 \rangle$ approximant. (*b*) The $\langle 1/1 \rangle$ approximant. (*c*) Two unit cells of the mercury crystal with the threefold axis directed along a threefold axis of the cubes in (*a*) and (*b*). The *L* and *S* atoms, shown by large and small circles, may be of the same kind. All closest neighbours of each atom are positioned at the vertices of a dodecahedron; to simplify the pictures, only visible edges of the dodecahedra are shown in (*a*) and (*c*) by dashed lines. For the $\langle 1/1 \rangle$ approximant, the DLO description seems to be trivial because the cube can always be inscribed into a dodecahedron; however, it is convenient to have such a unified description for all approximants.

In crystallographic books, this structure is referred to as a *B*20 or FeSi-type structure. It is found in many alloys: MnSi, AlMnSi, CoGeSi, GeRu, HfSn, HgPd and others (Villars & Calvert, 1985). In real crystals, atoms are slightly shifted from their ideal positions (see Table 1 and § 9). Note that, if *L* and *S* atoms are the same, then the space group of the idealized structure is *Pa*3 and we have the $\langle 2/1 \rangle$ approximant of a *primitive* icosahedral quasicrystal. If *L* and *S* atoms are different (as in all known alloys with the *B*20 structure), then the space group is $P2_13$ and we have the $\langle 2/1 \rangle$ approximant of a *face-centred* icosahedral quasicrystal (see discussion in § 7).

Pyrite-like crystals present a slightly different structure of the $\langle 2/1 \rangle$ approximant. The difference is that the centre of the prolate rhombohedron is occupied by an interstitial atom. This atom shifts other atoms from their ideal positions but perhaps stabilizes the structure. In Table 1, the atomic coordinates are given for a high-pressure form of PdF_2, where the shifts are very small (Tressand, Soubeyroux, Touhara, Demazeau & Langlais, 1981); in other pyrites they are more pronounced and DLO is less evident. To avoid confusion, it should be noted that the pyrite cubic structure has the origin shifted to $(\frac{1}{2},\frac{1}{2},\frac{1}{2})$ in comparison with the FeSi structure. Usually, in pyrites, *L* and *S* atoms are of the same sort, the space group is $Pa\bar{3}$ and we have the approximant of a

Table 1. *Positions of atoms and icosahedral holes in cubic approximants with DLO*

The hole marked by an asterisk is not icosahedral. Experimental values are given for the first compound of each approximant; for α-AlMnSi we take those positions that are less distorted by the atoms in the i-holes.

Label	Examples	Elser-Henley notations	Theoretical (x,y,z) coordinates in a unit cell	Experimental (x,y,z) coordinates in a unit cell	$(N_b' N_b N_c)$ or $(N_a' N_a)$	Six-dimensional indices
$\langle 1/1 \rangle$	FeSi	1/−1	(0,0,0)	(0,0,0)	(068)	000000
	AlPd		(0.5,0.5,0.5)	(0.5,0.5,0.5)	(068)	000$\bar{1}\bar{1}\bar{1}$
$\langle 2/1 \rangle_a$	FeSi	0/1	(0.845,0.845,0.845)	(0.844,0.844,0.844)	(067)	111000
	AlPd		(0.155,0.155,0.155)	(0.136,0.136,0.136)	(067)	000000
$\langle 2/1 \rangle_b$	PdF_2	0/1	(0.345,0.345,0.345)	(0.343,0.343,0.343)	(067)	000111
	FeS_2		(0.655,0.655,0.655)	(0.657,0.657,0.657)	(067)	000000
	Pyrites		(0,0,0)	(0,0,0)	-	*hole
$\langle 3/2 \rangle$	Au_3NaSi	1/0	(0.095,0.095,0.095)	(0.097,0.097 0.097)	(067)	000000
	Au_3NaGe		(0.214,0.095,0.405)	(0.226,0.133,0.408)	(066)	001000
			(0.405,0.405,0.405)	(0.381,0.381,0.381)	(39)	i-hole
$\langle 5/3 \rangle_a$	Al_5Li_3Cu	1/1	(0.191,0.191,0.191)	(0.187,0.187,0.187)	(067)	000000
	$Mg_{32}(AlZn)_{49}$		(0,0.118,0.191)	(0,0.094,0.154)	(075)	0$\bar{1}$0000
	$Au_4Na_3Si_2$		(0,0.309,0.118)	(0,0.305,0.117)	(076)	0$\bar{1}$0$\bar{1}$00
	Au_3Na_2Sn		(0.118,0.191,0.382)	(0.157,0.190,0.406)	(066)	00000$\bar{1}$
			(0.427,0,0.5)	(0.404,0,0.5)	(156)	$\bar{1}$100$\bar{1}$2
			(0.191,0,0.5)	(0.199,0,0.5)	(058)	$\bar{1}$01001
			(0.191,0.309,0)	(0.175,0.301,0)	(39)	i-hole
			(0,0,0)	(0,0,0)	(0,12)	i-hole
$\langle 5/3 \rangle_b$	α-AlMnSi	1/1	(0.118,0.191,0.309)	(0.115,0.187,0.300)	(076)	000000
	α-AlFeSi		(0.5,0.191,0.309)	(0.5,0.180,0.308)	(067)	100$\bar{1}$00
	$Sc_{57}Rh_{13}$		(0.5,0.118,0.118)	(0.5,0.120,0.117)	(065)	10$\bar{1}\bar{1}$00
	$Hf_{54}Os_{17}$		(0.118,0.118,0.118)	(0.164,0.100,0)	(067)	00$\bar{1}$000
			(0.5,0.5,0.118)	(0.5,0.5,0.122)	(156)	111$\bar{1}\bar{1}$0
			(0,0,0.236)	?	(156)	$\bar{1}$00010
			(0,0,0)	?	(068)	00$\bar{1}$111
			(0.309,0,0.5)	(0.290,0,0.5)	(2,10)	i-hole

primitive quasicrystalline lattice. However, the ordered form of this structure, which can be considered as an approximant of a face-centred quasicrystal, was also found (CoAsS, NiSbS, LaIrSi *etc.*). Pyrite is known for the almost dodecahedral form of its monocrystals. Mackay (1986) was the first to recognize pyrite as an approximant but he suggested other values for the atomic coordinates.

The smaller approximant, $\langle 1/1 \rangle$, can also occur in both the ordered form (CsCl structure) and the disordered form (b.c.c. structure). All shortest L–S bonds are directed along eight common cube and dodecahedron threefold axes. Because the ratio of lattice constants of the succeeding approximants is equal to τ, the cube in Fig. 1(*b*) can be exactly inscribed into the coordination dodecahedron in Fig. 1(*a*) and the dodecahedron can be inscribed into the cube in Fig. 1(*a*). Many alloys exhibit both modifications, shown in Figs. 1(*a*) and (*b*), with practically the same density of atoms (AlPd, AlPt, FeSi, OsSi and others). The close relationship between the two structures becomes more evident if we compare the oblate rhombohedra in both figures; they are equal but look different because they have different orientations relative to cubic axes. Hence, inside the lower-order $\langle 1/1 \rangle$ approximant we can find the whole unit cell (eight atoms) of the next $\langle 2/1 \rangle$ approximant. Such a relationship can be used for the construction of ever larger approximants (Dmitrienko, 1993).

The crystalline structure of the mercury exhibits one more example of DLO (see Fig. 1*c*). The rhombohedral unit cell of the mercury crystal is very close to the prolate rhombohedron shown in Fig. 1(*a*) and it is far from the rhombohedron of the f.c.c. packing; different sources give the mercury rhombohedral angle α_{Hg} between 70° 31′ and 70° 44′. Six closest neighbours of every atom are near to six vertices of the coordination dodecahedron and the centres of symmetry coincide with the atomic position. The next atomic shell is a hexagon of six atoms in the plane normal to the threefold axis; the distance to these atoms is $2/3^{1/2}$ times larger than the distance to the closest neighbours (like in $\langle 2/1 \rangle$ and $\langle 1/1 \rangle$ approximants). It is not clear yet whether the mercury crystal is a rhombohedral approximant of quasicrystals.

3. DLO in higher approximants and quasicrystals

Further examples of DLO can be found in larger approximants of quasicrystals (see Table 1). We can say that the approximants are DLO networks of atoms. The general methods of the construction of the DLO approximants with ever larger unit cells were discussed by Dmitrienko (1992, 1993); the generic property is that any approximant contains the representative pieces of smaller and larger approximants. Here, we should note several additional features that occur in the higher approximants in comparison with the smaller ones. The first and most evident feature is the existence of the atomic positions with different symmetry and different environments. The analysis of all possible local environments is beyond the scope of this paper; in Table 1 we present (for each site)

only the numbers of neighbouring atoms from the same DLO network. N_c is the number of closest neighbours at the threefold distance c_{-3} (DLO neighbours), N_b is the number of atoms at the twofold distance b_{-3} and N_b' is the number of atoms at the short frustrated distances b_{-3}/τ (such close bonds are also a typical feature of higher approximants - see § 9).

Another interesting phenomenon is the presence of interstitial atomic sites, marked as 'i-holes' in Table 1, which are the icosahedrally coordinated positions between the atoms of the DLO networks. All the closest atoms around an i-hole are positioned in pseudo-fivefold $\langle 10\tau\rangle$ directions but their distances from its centre are different: there are N_a neighbours at the normal interatomic distance a_R/τ and N_a' neighbours at the abnormally short distance a_R/τ^2. If we try to continue the dodecahedral arrangement inside i-holes, any new atomic position is too close to one of the old positions. Therefore, i-holes may be considered as the places of frustration for the DLO. In real crystals, the i-holes may be occupied by the atoms or may be empty.

The $\langle 3/2\rangle$ approximant is exemplified by Au_3NaSi and Au_3NaGe crystals; their space group is $Pa3$ with 40 atoms per unit cell: eight Na atoms [in 8(c) positions (x,x,x)] and 24 Au atoms [in the general 24(d) positions (x,y,z)] build up the DLO network, whereas eight Si or Ge atoms [in (x,x,x) positions] occupy the i-holes. The calculated values of the atomic coordinates are

$$\begin{gathered} x_{\mathrm{Na}} = 1/4\tau^2, \\ (x_{\mathrm{Au}}, y_{\mathrm{Au}}, z_{\mathrm{Au}}) = (5^{1/2}, 1, \tau^3), \\ x_{\mathrm{Si}} = \tau/4. \end{gathered} \tag{2}$$

The structure of the $\langle 3/2\rangle$ approximant is similar to that suggested by Kuriyama, Long & Bendersky (1985) (except for the atoms in the i-holes); I am grateful to a referee of a previous paper (Dmitrienko, 1993) who attracted my attention to this similarity.

The next approximants, $\langle 5/3\rangle_a$ and $\langle 5/3\rangle_b$, are close to the most popular crystals in quasicrystallography, Al_5Li_3Cu and α-AlMnSi; the space symmetry of both approximants is $Im\bar{3}$. As for the smaller approximants, the coordinates of atomic sites are simple functions of τ: $1/(2\tau) \simeq 0.309$, $1/2(\tau^2) \simeq 0.191$, $1/2(\tau^3) \simeq 0.118$ *etc.* Most of the atoms are in DLO networks and again there are i-holes. Per unit cell, the $\langle 5/3\rangle_a$ ($\langle 5/3\rangle_b$) approximant contains 136 (138) positions in the DLO network and 26 (12) positions in the large i-holes. In the $\langle 5/3\rangle_b$ approximant, the number of positions seems to be too large for real α-AlMnSi; some of them may be omitted (or partly occupied) to produce the observed $Pm\bar{3}$ symmetry of α-AlMnSi (Cooper & Robinson, 1966) and $Sc_{57}Rh_{13}$ as well as the $Immm$ symmetry of $Hf_{54}Os_{17}$ (Cenzual, Chabot & Parthé, 1985). The (0,0,0) i-hole is empty in Al_5Li_3Cu but it is occupied in Au_3Na_2Sn and in $Mg_{32}(AlZn)_{49}$ (Bergman, Waugh & Pauling, 1957) whereas other i-holes are occupied in all known cubic approximants of this order, enforcing small shifts of neighbouring atoms.

Note that (0.164,0.100,0.000) positions, which produce small empty icosahedra centred at (0,0,0) and $(\frac{1}{2},\frac{1}{2},\frac{1}{2})$ points in the conventional model of α-AlMnSi (Cooper & Robinson, 1966), correspond to the i-holes of the $\langle 5/3\rangle_b$ approximant [their theoretical coordinates are (0.191,0.118,0)]. However, neutron diffraction shows that such positions are absent in the AlMnSi quasicrystals (Janot, Dubois, Pannetier, de Boissieu & Fruchart, 1988). Therefore, and because of some theoretical arguments, we replace those empty icosahedra by the CsCl-type cubic arrangement of atoms, restoring the DLO network in those parts of the structure (like in Fig. 1*b*, see also §8). After such replacement, the intensities of X-ray and neutron reflections should not vary too strongly. It would be interesting to prove which model better fits the experimental data.

In the DLO model, there is a surprising duality between $\langle 5/3\rangle_a$ and $\langle 5/3\rangle_b$ structures. Indeed, in addition to the i-holes listed in Table 1, there are a lot of other i-holes in any DLO network; all the i-holes can be considered as projections of body-centre points of a six-dimensional lattice in the projection scheme described in §4. The i-holes themselves can produce a DLO network. It is easy to show that the positions of some i-holes in the $\langle 5/3\rangle_a$ approximant just correspond to atomic positions in the $\langle 5/3\rangle_b$ approximant and *vice versa*; for complete correspondence, the atomic coordinates (say, x and y) should also be permuted because of the convention on the direction of cubic axes in the $Im\bar{3}$ space group. In the $\langle 2/1\rangle$ and $\langle 3/2\rangle$ approximants, the same duality operation preserves their structures but shifts the origins of the unit cells.

4. Projection scheme for DLO

There are 20 places (20 vertices of the coordination dodecahedron) where we can find the closest neighbours of any atom of the DLO networks. 20 vectors, connecting the neighbours, have the following forms: eight (111) vectors and twelve $(01\tau^2)$ vectors (we use the Cartesian coordinates with the axes directed along cubic axes of approximants). Among those vectors we can select six independent vectors, $\mathbf{e}_1, \ldots, \mathbf{e}_6$; for example, we can take the vectors directed from the site 0 to six close neighbours, marked 1 to 6 in Fig. 1(*a*);

$$\begin{aligned} \mathbf{e}_1 &= \lambda_n(\tau^2, 0, 1), \\ \mathbf{e}_2 &= \lambda_n(1, \tau^2, 0), \\ \mathbf{e}_3 &= \lambda_n(0, 1, \tau^2), \\ \mathbf{e}_4 &= \lambda_n(-\tau^2, 0, 1), \\ \mathbf{e}_5 &= \lambda_n(1, -\tau^2, 0), \\ \mathbf{e}_6 &= \lambda_n(0, 1, -\tau^2), \end{aligned} \tag{3}$$

where the common factor depends on the order n of the approximant ($\lambda_n = \tau^{-n}/2$). All three-dimensional coordinates are given as fractions of the unit-cell dimensions; because $a_n \propto \tau^n$, the real length of the vectors is the same for all approximants. Then, we can express the position $\mathbf{r}_n$ of the nth atom of the DLO network as a sum of those six vectors with integer coefficients $n_1, \ldots, n_6$:

$$\mathbf{r}_n = n_1\mathbf{e}_1 + \ldots + n_6\mathbf{e}_6, \qquad (4)$$

but not all sets of integers are permitted.

As usual, it is convenient to consider six integers $n_1, \ldots, n_6$ as the coordinates of vertices in a six-dimensional cubic lattice, so that six vectors $\mathbf{e}_1, \ldots, \mathbf{e}_6$ are the projections of six edges of the cube onto our space. The numbers n_i are not independent; they are restricted by some strip in the six-dimensional space. We should select the size, direction and shape of the strip (i) to provide the icosahedral symmetry of quasicrystals and desirable symmetry of approximants and (ii) to prevent too short distances between atoms (details will be published elsewhere).

Such a projection scheme is a modification of the conventional strip-projection method (Kalugin, Kitaev & Levitov, 1985): the edges of a six-dimensional cube are projected on the *threefold* directions instead of the *fivefold* ones. The conventional fivefold basic vectors are the linear combinations of the threefold vectors given by (3) and *vice versa*; therefore, the global icosahedral symmetry of quasicrystals can be reached within both schemes. The DLO networks can be obtained within conventional projection schemes if some special decoration is used (see, for example, Cornier-Quiquandon, Quivy, Lefebre, Elkaim, Heger, Katz & Gratias, 1991).

By our method, we can obtain the six-dimensional coordinates for all atoms in any DLO network as is shown in Table 1 [for the $\langle 3/2\rangle$ and $\langle 5/3\rangle_a$ approximants, the x and y components of the basic vectors in (3) should be permuted]. Note that we use no special decoration of the six-dimensional lattice: atomic positions correspond to the projections of the vertices. The i-holes in the DLO networks have the half-integer six-dimensional coordinates; hence, they correspond to the projections of body centres of a six-dimensional cubic lattice.

5. Atomic size canonical cells

Originally, four canonical cells (A, B, C and D) were used for the description of a network of icosahedral nodes in quasicrystals and their large approximants (Henley, 1991). The cells consist of the nodes connected by two allowed kinds of linkage, called c (in the threefold direction) and b (in the twofold direction), where

$$c = \tau^2 a_R\left[3/\left(1+\tau^2\right)\right]^{1/2} \qquad (5)$$

and the b linkage is 15% longer,

$$b = \tau^2 a_R\left[4/\left(1+\tau^2\right)\right]^{1/2} \qquad (6)$$

(a_R is the usual quasilattice constant; in real alloys, $a_R \simeq 5$ Å and b and c are about 10 Å).

It is evident from Fig. 2 that small approximants can be constructed from small atomic size canonical cells. Their linear dimensions are τ^3 times *smaller* than the original ones:

$$c_{-3} = c\tau^{-3}; \quad b_{-3} = b\tau^{-3}. \qquad (7)$$

Hence, the lengths of the edges of the cells, c_{-3} and b_{-3}, are approximately typical interatomic distances.

For such small cells, we use the notations A_{-3}, B_{-3} and C_{-3}. Two of the cells, A_{-3} and C_{-3}, are slightly irregular tetrahedra; such configurations are favourable for four atoms and the distortions of the tetrahedra may be a result of a difference between atomic radii. If L and S atoms are different, we have two types of B_{-3} and C_{-3} cells but only one type of A_{-3} cell. The cells can match one another with rather obvious matching rules (Henley, 1991). The prolate rhombohedron (see Fig. 1) consists of two B_{-3} and two C_{-3} cells, whereas the oblate rhombohedron consists of six A_{-3} cells.

The small canonical cells fit the typical atomic arrangements and fill up most of the volume of approximants and quasicrystals. Nevertheless, it is impossible to describe *all* the local configurations with three or even four small cells [we can introduce the fourth cell, D_{-3}, which can be found in the $\langle 3/2\rangle$ approximant; it is τ^3 times smaller than the D cell found by Henley (1991)]. The most obvious place where it is impossible is the empty icosahedron centred at the (0,0,0) positions in the $\langle 5/3\rangle_a$ approximant. Another place is near the (0.5,0,0.5) point in the the same structure: there are two equivalent atomic sites, (0.427,0,0.5) and (0.573,0,0.5), separated by an abnormally small distance b_{-3}/τ (in a real crystal the atoms are shifted out to a normal distance). The similar short bond is between the (0,0,0.236) and (0,0,0.382) positions in the $\langle 5/3\rangle_b$ approximant.

There are two possible solutions to this problem. The first is to add new cells to describe all such places, but

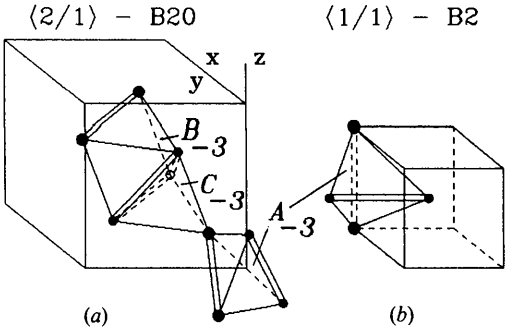

Fig. 2. The atomic size canonical cells A_{-3}, B_{-3} and C_{-3} in the small cubic approximants (*a*) $\langle 2/1\rangle$ and (*b*) $\langle 1/1\rangle$. Single and double lines correspond to the (pseudo-)threefold c_{-3} bonds and the (pseudo-) twofold b_{-3} bonds, respectively.

their number is too large to be constructive. For instance, we can add (i) the D_{-3} cell and (ii) the icosahedron of 12 atoms connected by 30 b_{-3} bonds *etc.* It might be useful to enumerate all the places of this type because such places may be important for phason-type reconstructions, but this is beyond the scope of this paper. The second, more reasonable, solution is to consider all 'bad' places as the places where canonical-cell ordering is frustrated (this is further discussed in § 9).

6. DLO-induced decorations for the Ammann rhombohedra and for the canonical cells

It is interesting to understand the relationship between DLO ordering and the traditional description of icosahedral quasicrystals. Namely, what is the DLO-induced decoration of the Ammann rhombohedra, the canonical cells and other units usually used for quasiperiodic tilings? To answer this question, we should find these units inside the known approximants with DLO. Surprisingly, two different decorations of the Ammann rhombohedra were found in the same $\langle 2/1\rangle_a$ approximants (Fig. 3): (i) the edge decoration; (ii) the vertex-face decoration.

In the case of the edge decoration, the prolate and oblate Ammann rhombohedra are centred in the (0,0,0) and $\left(\frac{1}{2},\frac{1}{2},\frac{1}{2}\right)$ positions and their threefold axes are parallel to the cubic threefold axes. Each edge (its length is a_R) is divided by the atomic site in the golden ratio. Two atomic sites at the body diagonal of the prolate rhombohedron divide the diagonal in the ratios $\tau{:}1{:}\tau$. If L and S atoms are of the same kind, the rhombohedra can match face to face; in the $B20$ structure, they interpenetrate because this approximant is too small. If L and S atoms are different, the decorated rhombohedra are chiral: they have two forms, left and right, which are mirror reflections of each other; the chiral rhombohedra can match face to face only with the rhombohedra of opposite chirality [in Fig. 3(*a*), the prolate and oblate rhombohedra are of the same chirality]. The vertices of the rhombohedra correspond to the i-holes; in higher approximants, they can be occupied (at least partly) by the interstitial atoms shifting the edge atoms from their ideal positions to the middles of the edges. After such shifts, the decoration becomes similar to that one usually used for AlLiCu quasicrystals (Hiraga, Hirabayashi, Inoue & Masumoto, 1985).

Another choice of the positions of the rhombohedra (the prolate one in the centre and the oblate one in the origin) gives the vertex-face decoration (Fig. 3*b*). We see that a_R is the minimal fivefold distance in the DLO networks. The atoms on the faces divide the long face diagonals in the golden ratio. Two atoms at the body diagonal of the prolate rhombohedron divide it into three segments in the ratio $1{:}5^{1/2}{:}1$. Note that the body diagonal of the oblate rhombohedron is a c_{-3} bond whereas the body diagonal of the prolate rhombohedron is τ^3 time longer, that is, it is equal to the c linkage (Henley, 1991). The decorated rhombohedra are not chiral and they can match face to face even if L and S atoms are different. This decoration is similar to that used for AlMnSi quasicrystals (Elser & Henley, 1985; Janot, Dubois, Pannetier, de Boissieu & Fruchart, 1988).

In higher approximants, the decorations of the Ammann rhombohedra may have some changes (the body-diagonal sites may be unoccupied like in the $\langle 3/2\rangle$ approximant, some i-holes may be filled by atoms *etc.*) but we have not found new types of decorations compatible with DLO.

As for the canonical cells, their atomic decorations can be found in several ways. Firstly, we can find decorated A, B, C and D cells in the $\langle 5/3\rangle$, $\langle 8/5\rangle$ and $\langle 13/8\rangle$ approximants, correspondingly τ^3 inflated in comparison with the $\langle 1/1\rangle$, $\langle 2/1\rangle$ and $\langle 3/2\rangle$ approximants. Unfortunately, the real atomic structures and their DLO idealizations are not known for the $\langle 8/5\rangle$ and $\langle 13/8\rangle$ approximants; hence, only the decorations of the A cell

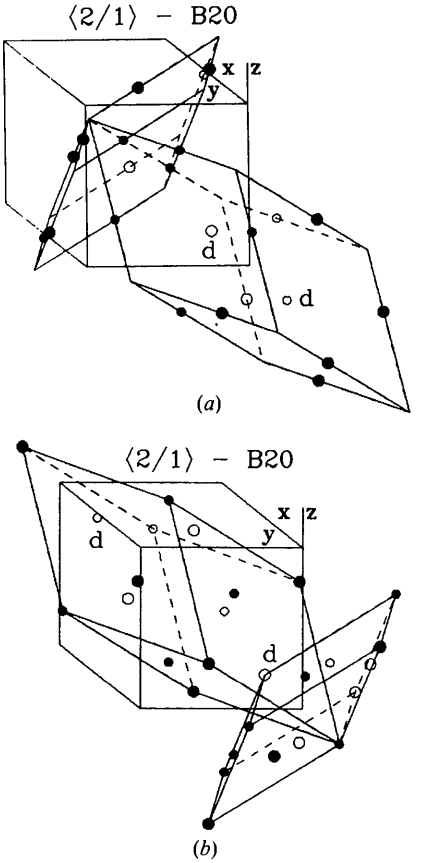

Fig. 3. Two different DLO-induced decorations of the Ammann rhombohedra in the same cubic approximant, $\langle 2/1\rangle_a$: (*a*) the edge decoration; (*b*) the vertex-face decoration. All the edges of the Ammann rhombohedra are directed along pseudo-fivefold axes. Large and small circles represent the L and S atoms, respectively; the letter d marks atoms at the body diagonals of the prolate Ammann rhombohedra. The cubes designate the unit cell of the $B20$ structure.

can be found this way (inside the $\langle 5/3 \rangle$ approximants). Secondly, we can use the relations of the canonical cells to the Ammann rhombohedra, as given by Henley (1991), plus the DLO decorations of the letters, found above. Thirdly, we can combine the symmetry of the canonical cells (Henley, 1991) and DLO; it is evident that only a few decorations meet both these conditions.

Then, by the second or third method, we can obtain (at least, in principle) the next generation of the cells, τ^3 larger than canonical cells, and so on *ad infinitum*. Cubic approximants of any high order (but not all of them!) can be constructed if we replace the atomic size canonical cells in $\langle 1/1 \rangle$, $\langle 2/1 \rangle$ and $\langle 3/2 \rangle$ approximants by the ever larger canonical cells.

7. Even/odd ordering in DLO networks

It is well known that some alloys may exist both in an ordered (CsCl type) phase and in a disordered (b.c.c.) phase, and there may be a phase transition between these phases. The same phenomenon is possible in other DLO networks as well. Atoms in any DLO network can be divided into even and odd sublattices wherein neighbours related by c_{-3} bonds have opposite parities, while those related by b_{-3} bonds have the same parity. If the atoms of even and odd sublattices are different, then we have even/odd ordering in DLO networks. For instance, all the structures shown in Figs. 1 and 2 can be divided into subsets of L and S atoms; the ordered (disordered) phase corresponds to $L \neq S$ ($L = S$). For neighbouring atoms, such ordering is a very typical feature of many alloys. At larger scales, the even/odd ordering of DLO networks produces the even/odd ordering of icosahedral nodes, considered by Henley (1991), because any c linkage is a sum of an *odd* number of c_{-3} bonds (more exactly, the sum of an odd number of $\mathbf{e}_i$). We can also assign a parity to i-holes because each i-hole is surrounded by the atoms of the same parity; in the conventional model of the α-AlMnSi crystal, the i-holes of some parity are occupied by atoms whereas the holes of opposite parity are empty. It should be noted here that all typical threefold and fivefold distances ($\tau^{3k} c_{-3}$ and $\tau^{3k} a_R$, where $k = 0, 1, 2, 3, \ldots$) are sums of odd $\mathbf{e}_i$, whereas the typical twofold distances ($\tau^k b_{-3}$), which are also the periods of cubic approximants, are the even sums of $\mathbf{e}_i$.

In the six-dimensional cubic lattice, the transition from $L = S$ to $L \neq S$ is the transition from the primitive lattice (with one atom per cell) to the f.c.c. (NaCl-like) lattice (Henley, 1988; Niizeki, 1990). Therefore, when $L = S$, all cubic approximants that are considered are the approximants of quasicrystals with primitive lattices, whereas, when $L \neq S$, they are the approximants of face-centred quasicrystals. According to the Landau theory (Landau & Lifshitz, 1968), in some cases such a phase transition may be of the second order but in other cases modulated structures can arise; a detailed discussion of this will be given elsewhere. Note that the diffuse reflections frequently observed in the quasicrystals with the primitive lattice may be a result of the even/odd short-range (middle-range) ordering.

The $\langle 1/1 \rangle$ and $\langle 2/1 \rangle$ approximants were observed both in ordered and in disordered forms; corresponding space groups are $Pm\bar{3}m$ and $Im\bar{3}m$ for the $\langle 1/1 \rangle$ approximant, whereas for the ordered $\langle 2/1 \rangle_a$ approximant the space group is $P2_13$ and for the disordered $\langle 2/1 \rangle_b$ approximant it is $Pa3$. In $\langle 5/3 \rangle$ approximants, the ordering of this type leads to a transition from $Im\bar{3}$ to $Pm\bar{3}$ symmetry; we can speculate that the $Pm\bar{3}$ symmetry of α-AlMnSi may be a result of such ordering (contrary to the conventional point of view, which considers the $Pm\bar{3}$ symmetry to be a result of the partial occupancy of i-holes). There is experimental evidence (Dubois, Kang & von Stebut, 1991) that $Al_{65}Cu_{20}Fe_{15}$ quasicrystals (usually face centred) can exist in the disordered primitive phase as well. It is worth noting that in large approximants ($\langle 3/2 \rangle$ and larger) there is additional ordering of chemically different atoms that cannot be described within the present DLO model; a more complicated approach is perhaps needed (see § 10).

Special attention should be paid to the notation of the cubic approximants of the face-centred quasicrystals. It has been shown (Dmitrienko, 1990) that all three-dimensional Miller indices of these approximants are even; formally, we have the face-centred cubic approximants, which should be labelled $\langle 2F_{n+1}/2F_n \rangle$. However, we can (in fact *must*) choose a new cubic unit cell that is half as large in all directions. After such a choice, we have the same size of unit cell, the same Miller indices of the common Bragg reflections and the same notation $\langle F_{n+1}/F_n \rangle$ for the cubic approximants of primitive and face-centred quasicrystals (but of course they have different space groups). The three-dimensional indices of the superlattice reflections (in approximants of the face-centred quasicrystals) are also integers. It is convenient to have such a unified description, as it is convenient to use the same unit cell for CsCl and b.c.c. structures. The only disadvantage of this convention is that the six-dimensional indices of superlattice reflections are semi-integers.

8. Physical reasons for the dodecahedral local ordering

At first glance, it seems rather mysterious that atoms are positioned in the vertices of dodecahedra. Now, we want to show that DLO is naturally produced by the b.c.c. and CsCl-type atomic ordering. First of all, we compare b.c.c. and mercury lattices (Fig. 4). The (001) atomic plane of the mercury crystal is very close to the (110) plane in the b.c.c. crystal because the rhombohedral angle in mercury is close to 70° 32′ (Fig.

4). However, there is different stacking of those planes in the perpendicular direction: in the b.c.c. structure, the next plane is shifted at half of the period in the [110] direction; in the mercury crystal, the shift is twice as small (compare Figs. 4*a* and *b*). Each subsequent plane produces a layer of the oblate rhombohedra in the b.c.c. structure and a layer of the prolate rhombohedra in the mercury structure. Comparing Figs. 4(*a*) and (*b*), we can see that the b.c.c. lattice and the mercury lattice are very close and that one structure can be transformed into the other by a rather small shift of the upper plane as a whole. It is interesting that such a martensitic transformation may be a stage of a practically important b.c.c.-f.c.c. transition. Indeed, a mercury-like crystal can easily be transformed into a f.c.c. structure by decreasing the rhombohedral angle to 60°. Hence, instead of the classical Bain transformation, the b.c.c.-f.c.c. transition can proceed *via* the mercury-like intermediate state.

The second example (Fig. 5), closely related to the first one, demonstrates the generation of a cluster similar to the Mackay icosahedron. Let us consider the CsCl-like cluster of seven *S* and eight *L* atoms that can be divided into four oblate rhombohedra or 24 A_{-3} cells [see Fig. 5(*a*) and compare it with Fig. 1(*b*)].

We suppose that the interatomic distances have the following values favourable for the CsCl-type ordering:

$$r_{LL} = b_{-3}; \quad r_{SS} < r_{LL}; \quad r_{LS} = c_{-3}. \qquad (8)$$

It should be particularly emphasized that we fix only the lengths of interatomic bonds, not their directions.

Now, we try to find favourable places for new additional atoms in the next coordination sphere. Usually, the favourable places are at the vertices of the tetrahedra where a new atom contacts with three old atoms. To continue the CsCl-like structure, we should add an *S* atom (marked *S'* in Fig. 5*a*). If instead of the *S* atom we add an *L* atom (marked *L'*) and if the new *L* atom is at typical distances from its neighbours [(8)], then it is easy to see that the *L* atom has the position $(\frac{\tau^2}{2}, \frac{\tau}{2}, 0)$ (all the coordinates are in fractions of the unit-cell dimensions). This position is in a pseudo-threefold $[1\tau^2 0]$ direction relative to the closest *S* atom and in a pseudo-fivefold $[\tau 10]$ direction relative to the central *S* atom. In other words, the additional *L* atom forms a C_{-3} cell on the face of an A_{-3} cell. There may be several reasons to prefer an *L* atom to an *S* atom, either energetic (if an *L* atom is energetically favourable to this coordination sphere) or statistical (if there are more *L* atoms in the cluster environment).

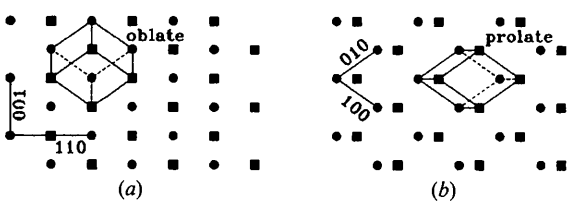

Fig. 4. Stacking of the similar atomic planes in (*a*) b.c.c. and (*b*) mercury crystals. The first plane is shown as circles and the second as squares.

As the next step, we can fill another place of the same type in the vicinity of the same *S* atom (it is impossible to occupy two others because they would be too close to the first *L* atom). These two places reduce the symmetry from fourfold to twofold. A dozen *L* atoms in such positions form a regular icosahedron around the centre of the cluster [$(\frac{\tau^2}{2}, \frac{\tau}{2}, 0)$ positions] and complete this coordination sphere (Fig. 5*b*).

To fill the next coordination sphere with the same packing rules, we should add 24 *S* atoms at the vertices of A_{-3} tetrahedra, formed on the faces of those C_{-3} cells that were created at the previous stage. These atoms are at pseudo-twofold $(\frac{1}{2}, \frac{\tau^2}{2}, \frac{\tau}{2})$ positions relative to the central atoms; their distances from the central atom are equal to τ. One of them is marked as *S''* in Fig. 5(*b*). Note, that the B_{-3} cells occur automatically at this stage.

Thus, starting from the 15-atom CsCl-like cluster, we created the 51-atom cluster with the dodecahedral local arrangement of all atoms. If we add six atoms in $(\tau,0,0)$ positions, then the symmetry of the outer shell of the cluster becomes icosahedral (Fig. 5*c*) and we obtain just that cluster that surrounds the centre of coordinates in the $\langle 5/3 \rangle_b$ approximant (see Table 1). However, each of these new atoms has one abnormally short bond (marked by crosses in Fig. 5*d*) with an old atom. This is a typical frustrated place as discussed in § 9. Note that the outer shell of the cluster, grown in this manner, coincides with the outer shell of the Mackay icosahedron, whereas the inner parts are different.

From these examples, we see that the packing of the matched A_{-3} and C_{-3} tetrahedra naturally produces DLO and icosahedral motifs in large clusters; note also the densely populated atomic planes, which are normal to the twofold and pseudo-fivefold directions (see Fig. 5*c*). It seems that such a 'growth' of DLO clusters can be easily simulated with a computer.

Another physical argument for DLO arises from the maximum-density principle. For example, let us find what is the densest configuration of eight atoms in the cubic unit cell with $Pa\bar{3}$ symmetry if the minimal distance between atoms is fixed. The dimensionless coordinates of the atoms are (x,x,x), $(\bar{x},\bar{x},\bar{x})$, $(\frac{1}{2}+x,\frac{1}{2}-x,x)$ *etc.* To obtain the maximal density, we should find that x thst provides the maximum of the dimensionless distance between closest neighbours. It is easy to see that the maximum is reached when the distances to six closest neighbours of each atom just coincide with the distance to the seventh closest neighbour, that is

$$\left(\tfrac{1}{2} - 2x\right)^2 + \left(\tfrac{1}{2}\right)^2 = (2x)^2 + (2x)^2 + (2x)^2. \qquad (9)$$

From (9), we obtain $x = 1/(4\tau)$. Hence, that x which gives DLO in $\langle 2/1 \rangle$ approximants [see (1)] also pro-

vides a maximum of their atomic density. It would be interesting to apply this idea to higher approximants.

It is not very clear which interaction produces the DLO in the mercury crystal where all the atoms are of the same size. One possible explanation is that, just for that rhombohedral angle, which corresponds to the DLO, the Fermi surface of mercury touches simultaneously different faces, {011} and {111}, of the Brillouin zone; such events are of great importance for the structure of metallic crystals (Jones, 1960) and quasicrystals (Poon, 1992).

9. Some intrinsic distortions of DLO

The previous sections have demonstrated that we can create, either step by step or globally (with projection methods), large DLO networks. However, in such systems some specific distortions arise, perhaps inevitably; therefore, DLO should be treated as an idealization of real ordering: real structures have the DLO networks distorted for several reasons. First of all, most atoms have asymmetric environments and are shifted from ideal DLO positions if real interatomic interactions are taken into account. The small shifts of atoms in the $B20$ structure are an example of such distortion. Then, real quasicrystals are alloys of two or more sorts of atoms with different atomic radii; this also produces some shifts of atoms.

The more important cause of DLO imperfection is the presence of frustrated places of two types:

(i) the interstitial atoms that occupy i-holes and shift neighbouring atoms of the DLO network;

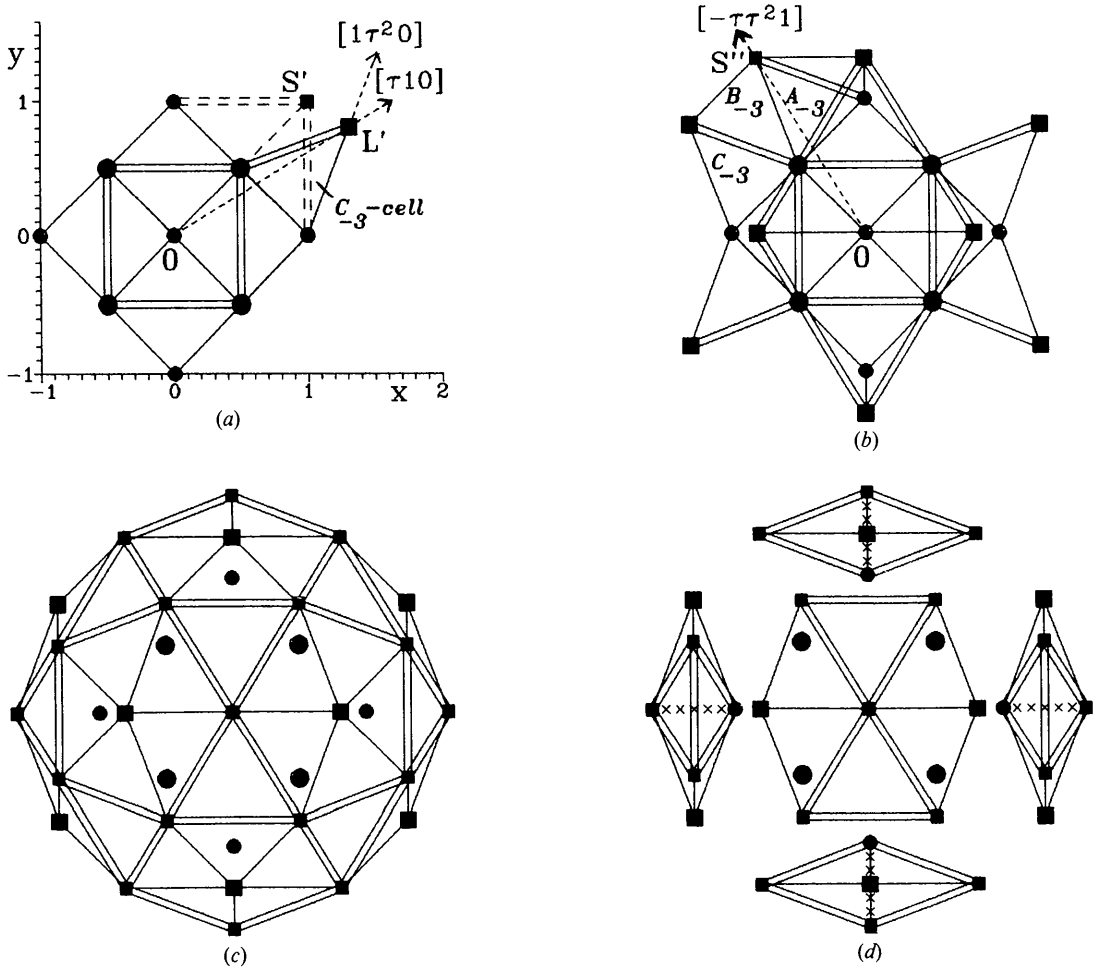

Fig. 5. Growth of an atomic cluster with dodecahedral and icosahedral motifs. Large circles or squares represent L atoms and small circles or squares S atoms. All atoms are projected on the xy plane and single and double lines are the projections of c_{-3} and b_{-3} bonds, respectively. The initial CsCl-like clusters are shown as circles whereas adjoining atoms are shown as squares; for simplicity, the evident b_{-3} bonds between small atoms of the initial cluster are not shown. (*a*), (*b*) and (*c*) The successive stages of the growth (see text). Note that the cluster in (*c*) is the modified Mackay icosahedron. (*d*) The frustrated pairs of atoms in the final cluster. The short frustrated bonds are marked by crosses. The closest neighbours of each atom are at the vertices of a small dodecahedron, as in Fig. 1 (except for the frustrated pairs of atoms).

(ii) the pairs of atoms connected by the short twofold bonds, b_{-3}/τ, which we call the close pairs [for such atoms $N_b' = 1$ in Table 1; Fig. 5(*d*) shows their typical environment in different projections].

In real crystals like Al_5Li_3Cu, such frustrated bonds relax to allowed interatomic distances. However, there is another way to escape frustration in such places if only one of two close sites is occupied by an atom. In the latter case, the frustrated places of the second type may be considered as a physical realization of the two-level system. Indeed, the atom can jump rather easily between two close sites through the ring of six neighbouring atoms (see Fig. 5*d*). In the $\langle 5/3\rangle_b$ approximant, two close sites are not equivalent; hence, their occupancies should be different. In the $\langle 5/3\rangle_a$ approximant, two close positions are crystallographically equivalent and their occupancy should be 0.5; this possibility cannot be ruled out even for the well investigated structure of Al_5Li_3Cu because it is difficult to distinguish one Al atom from half of a Cu atom in these positions.

As for the i-holes, it is not clear when they are occupied by atoms and when they are not. Note only that the occupied i-holes look like the 'wrongly inflated' positions of DLO. For instance, starting from the (0,0.118,0.191) position, we find the τ^3 inflated position, (0,0.5,0.809), in the DLO network of the $\langle 5/3\rangle_a$ approximant, whereas the τ-inflated site is the filled i-hole (0,0.191,0.309); the same phenomenon presents itself in the $\langle 5/3\rangle_b$ approximant.

Note also that the universal local arrangement of atoms (like DLO) should provoke other types of distortions: (*a*) easy twinning and (*b*) coherent growth of approximants and quasicrystals. From the real example (Fig. 3), we can see that the DLO-induced decorations make possible both the face-to-face matches of the Ammann rhombohedra and their intersections. The intersections may be important for the defect formation in quasicrystalline alloys. It seems that all the considered sources of distortions are intrinsic both to the DLO and (in τ_3 larger scales) to the CCO; they can generate at least a part of the observed disorder in quasicrystals.

10. Concluding remarks

The above consideration shows that the dodecahedral local ordering, which was originally found in small approximants (Dmitrienko, 1990), may be successfully used for larger approximants and quasicrystals. We have shown that on ever larger scales there are τ^3 inflated arrangements of threefold and twofold bonds; therefore, it seems better to speak about dodecahedral rather than icosahedral arrangements of atoms, nodes *etc.* in the quasicrystals and approximants (the node may be considered as a τ^3-inflated atom).

The τ^3-times reduced canonical cells (A_{-3}, B_{-3} and C_{-3}) give us a good opportunity to describe local atomic arrangements. Nevertheless, it is impossible to describe all local configurations with three or four small cells; the most evident place for which this is so is an empty icosahedron (i-hole) centred at the (0,0,0) positions in Al_5Li_3Cu (see § 9). It is not very clear how many different i-holes may arise in DLO networks but this number is not very large.

There may be several different cubic approximants of each order: they may be symmorphic or nonsymmorphic (Dmitrienko, 1987), even/odd ordered or disordered (§ 7); in some cases, we can obtain new structures using a duality operation (§ 3). But for each order the number of possible structures is finite if we demand that the DLO network should have cubic space symmetry. Thus, in principle, we can enumerate all possible cubic approximants of a given order; for noncubic approximants, DLO restricts the possible values of the lattice parameters.

Within the present DLO model, we can describe the transition between quasicrystals (approximants) with primitive and face-centred six-dimensional lattices (see §7). However, such a crude model is unable to describe the chemical ordering in large approximants ($\langle 3/2\rangle$ and larger). Nevertheless, we can speculate that more complicated ordering in the six-dimensional lattice (together with the DLO projection scheme) will be able to provide the real atomic compositions of approximants and quasicrystals.

There is another way to describe real atomic composition, which seems even more plausible than the cut-projection method with several atomic surfaces. Indeed, it is possible to use the strip-projection method with a simple six-dimensional lattice (primitive or face-centred) but to separate the three-dimensional atomic sites in accordance with their positions in the strip, that is, in accordance with their perpendicular coordinates. Roughly speaking, the positions near the strip centre and the positions near the strip boundary should correspond to different sorts of atoms in a three-dimensional (quasi)lattice. Or, in other words, the strip should be divided (in the orthogonal space) into several substrips corresponding to different sorts of atoms. Such an approach seems reasonable because for each site both the coordination number and symmetry of the site environment depend crucially on its perpendicular coordinates. If this idea is valid, there is an important consequence: occupying some site, the atom of the definite sort stabilizes the perpendicular coordinates of the site, restricts the phason motions and favours approximant structures rather than the quasicrystalline one.

The phason motion can be also restricted owing to the occupancy of icosahedral holes by interstitial atoms. Indeed, the icosahedral holes are just the places of low density where easy structural transformation of phason type can occur (Kléman, 1989); if the places are filled, the phason motions may be frozen.

It seems natural that the atomic structures with DLO should grow most quickly in the (pseudo-)threefold

directions (that is, in the directions towards the closest neighbours); therefore, it is not surprising that the three-fold faces are usually absent on the surfaces of growing quasicrystals.

The relationship between the icosahedral quasicrystals and the CsCl structure (*via* A_{-3} cells) was demonstrated above. Now, it is interesting to note that pieces of the (110) atomic plane of CsCl have been suggested by Dong, Dubois, Kang & Audier (1992) as the structural units for the *decagonal* phase. Perhaps this is an explanation for why the icosahedral, decagonal and CsCl-like phases have close compositions in many alloys.

The author is grateful to N. N. Devnina and E. Kuklina for their help in the bibliography search for crystal structures. At different stages of this work, discussions with M. A. Fradkin, R. V. Galiulin, M. Kléman, L. S. Levitov and H.-R. Trebin were very fruitful. The support of l'Université Pierre et Marie Curie (Paris VI), France, where the final part of the work was done, is acknowledged.

References

BERGMAN, G., WAUGH J. L. T. & PAULING, L. (1957). *Acta Cryst.* **10**, 254-259.
BOUDARD, M., DE BOISSIEU, M., JANOT, C., HEGER, G., BEELI, C., NISSEN, H.-U., VINCENT, H., IBBERSON, R., AUDIER, M. & DUBOIS J. M. (1992). *J. Phys. Condens. Matter*, **4**, 10149-10168.
CENZUAL, K., CHABOT, B. & PARTHÉ, E. (1985). *Acta Cryst.* **C41**, 313-319.
COOPER, M. & ROBINSON, K. (1966). *Acta Cryst.* **20**, 614-617.
CORNIER-QUIQUANDON, M., QUIVY, A., LEFEBRE, S., ELKAIM, E., HEGER, G., KATZ, A. & GRATIAS, D. (1991). *Phys. Rev. B*, **44**, 2071-2084.
DMITRIENKO, V. E. (1987). *Pis'ma Zh. Eksp. Teor. Fiz.* **45**, 31-34. Engl. Transl: *JETP Lett.* **45**, 38-42.
DMITRIENKO, V. E. (1990). *J. Phys. (Paris)*, **51**, 2717-2732.
DMITRIENKO, V. E. (1992). *Pis'ma Zh. Eksp. Teor. Fiz.* **55**, 388-391. Engl. transl: *JETP Lett.* **55**, 391-395.
DMITRIENKO, V. E. (1993). *J. Non-Cryst. Solids*, **153&154**, 150-154.
DONG, C., DUBOIS, J. M., KANG, S. S. & AUDIER, M. (1992) *Philos. Mag. B*, **65**, 107-126.
DUBOIS, J. M., KANG, S. S. & VON STEBUT, J. (1991). *J. Mater. Sci. Lett.* **10**, 537-541.
ELSER, V. & HENLEY, C. L. (1985). *Phys. Rev. Lett.* **55**, 2883-2886.
GUYOT, P., KRAMER, P. & DE BOISSIEU, M. (1991). *Rep. Prog. Phys.* **54**, 1373-1425.
HENLEY, C. L. (1988). *Philos. Mag. Lett.* **58**, 87-89.
HENLEY, C. L. (1991). *Phys. Rev. B*, **43**, 993-1020.
HIRAGA, K., HIRABAYASHI, M., INOUE, A. & MASUMOTO, T. (1985). *J. Phys. Soc. Jpn*, **54**, 4074-4080.
JANOT, C., DUBOIS, J. M., PANNETIER, J., DE BOISSIEU, M. & FRUCHART, R. (1988). *Quasicrystalline Materials*, edited by C. JANOT & J. M. DUBOIS, pp. 107-125. Singapore:World Scientific.
JONES, H. (1960). *Theory of Brillouin Zones and Electronic States in Crystals*. New York: Interscience.
KALUGIN, P. A., KITAEV, A. YU. & LEVITOV, L. S. (1985). *Pis'ma Zh. Eksp. Teor. Fiz.* **41**, 119-121. Engl. transl: *JETP Lett.* **41**, 145-149.
KLÉMAN, M. (1989). *Adv. Phys.* **38**, 605-667.
KURIYAMA, M., LONG, G. G. & BENDERSKY, L. (1985). *Phys. Rev. Lett.* **55**, 849-851.
LANDAU, L. D. & LIFSHITZ, E. M. (1968). *Statistical Physics*, 2nd ed. New York: Pergamon.
MACKAY, A. L. (1981). *Kristallografiya*, **26**, 910-919. Engl. transl: *Sov. Phys. Crystallogr.* **26**, 517-522.
MACKAY, A. L. (1986). *Scr. Metall.* **20**, 1205-1210.
NIIZEKI, K. (1990). *J. Phys. A*, **23**, L1069-L1072.
PENROSE, R. (1979). *Math. Intell.* **2**, 32-37.
POON, S. J. (1992). *Adv. Phys.* **41**, 303-363.
STEURER, W. (1990). *Z. Kristallogr.* **190**, 179-234.
TRESSAND, A., SOUBEYROUX, J. L., TOUHARA, H., DEMAZEAU, G. & LANGLAIS, F. (1981). *Mater. Res. Bull.* **16**, 207-214.
VILLARS, P. & CALVERT, L. D. (1985). *Pearson's Handbook of Crystallographic Data for Intermetallic Phases*, Vols. 1-3. Metal Park, Ohio: American Society of Metals.

Acta Cryst. (1994). A**50**, 526–537

The Heavy-Atom Problem: a Statistical Analysis. I. *A Priori* Determination of Best Scaling, Level of Substitution, Lack of Isomorphism and Phasing Power

BY PHILIPPE DUMAS

UPR de Biologie Structurale, Institut de Biologie Moléculaire et Cellulaire, 15 rue René Descartes, 67084 Strasbourg CEDEX, France

(*Received* 22 *September* 1993; *accepted* 7 *February* 1994)

Abstract

The classical problem of determining heavy-atom parameters in single or multiple isomorphous replacement methods is reconsidered in two related papers. This first paper systematically examines how to derive *a priori* statistical information concerning heavy atoms and lack of isomorphism (LOI). By *a priori* is meant without any knowledge other than that of the measured intensities (and their estimated σ's) of a 'native' and 'derivative' crystal pair, that is to say *before* any potential site of substitution has been determined. First, both the terms $\Sigma_H = \sum_{i=1}^{N} f_i^2$, where f_i is the scattering factor of the ith heavy atom and N is the number of sites and, simultaneously, the best scale factor between the 'native' and 'derivative' data are estimated *a priori* as